# Intensification of preexisting auroral arc at substorm expansion phase onset: Wave-like disruption during the first tens of seconds

Jun Liang,[1] E. F. Donovan,[2] W. W. Liu,[1] B. Jackel,[2] M. Syrjäsuo,[3] S. B. Mende,[4] H. U. Frey,[4] V. Angelopoulos,[4] and M. Connors[5]

Received 15 February 2008; revised 3 April 2008; accepted 8 April 2008; published 3 May 2008.

[1] With the deployment of the all-sky imager array of the THEMIS mission, we were able to construct a preliminary database of auroral substorm expansion phase onsets, from which we have established a number of common features characterizing the first tens of seconds of the substorm auroral intensification. We find that the intensification occurs within ~10 sec over an arc segment extending approximately 1 h MLT and featuring wave-like formations distributed in longitude. The longitudinal wave number ranges between 100 and 300 such that the wavelength is comparable to the ion gyroradius in the central plasma sheet. The scale the intensification is about 10–30 sec. This study casts important observational constraints on substorm onset theories. **Citation:** Liang, J., E. F. Donovan, W. W. Liu, B. Jackel, M. Syrjäsuo, S. B. Mende, H. U. Frey, V. Angelopoulos, and M. Connors (2008), Intensification of preexisting auroral arc at substorm expansion phase onset: Wave-like disruption during the first tens of seconds, *Geophys. Res. Lett.*, *35*, L17S19, doi:10.1029/2008GL033666.

## 1. Introduction

[2] The expansion phase (EP) of the substorm is marked by spectacular displays of aurora in the oval. The onset of the EP typically manifests itself in the ionosphere as a sudden brightening (or "breakup") of a preexisting arc, either being a long-standing growth phase arc or formed a couple of minutes prior to the onset [*Lyons et al.*, 2002]. Despite decades of observations and investigations, our understanding of the substorm onset dynamics remains incomplete. It is generally acknowledged that the cross-tail current disruption at the inner edge of the plasma sheet and the mid-tail reconnection are two fundamental components in the substorm process, but their temporal sequence and relative importance are highly controversial. Current disruption is generally attributed to some plasma instabilities in the near-geosynchronous plasma sheet (NGPS), but the key instability type dominating the onset process is still indeterminate [*Lui*, 2004].

[3] Substorm EP onset is violent and explosive. Many believe that the secret of substorm physics is locked in the tens of seconds surrounding the onset. To date, our attempts to answer the 10-second question have been hampered by the lack of global auroral observations of sufficiently high temporal resolution. The THEMIS mission contains a continent-wide all-sky imager (ASI) array which provides an unprecedented combination of mesoscale imaging at high time resolution. Preliminary results have shown that the THEMIS ASIs are capable of providing new information to substorm EP onset research [*Donovan et al.*, 2006a, 2006b; *Mende et al.*, 2007]. The high resolution THEMIS ASI observations allow us to establish the onset morphology and evolution in great detail, as well as much-needed observational constraints against which theoretical proposals are to be tested. In this paper, we report first results from a survey of THEMIS ASI data with an emphasis on a few tens of seconds around the onset. The underlying database contains eight substorms for which we have good viewing of the aurora throughout the onset region. In this paper we give the list of the eight events and present details of two of them, occurring on February 22, 2006 and January 27, 2006, respectively. From the two events one can glean both the commonality and variation of the perturbation pertinent to EP onset. Specifically we found that the onset perturbation emerges nearly simultaneously from a wave-like auroral structure extending 10–15° MLON. The longitudinal wave number of the perturbation is high ($m \sim 200$), with implied longitudinal wavelength in the equatorial plane comparable to proton gyroradius. Finally, the growth rate of the underlying instability inferred from auroral brightness is of the order of 10 s. We conclude the paper with a general discussion of the implications of our result for substorm EP onset theories.

## 2. THEMIS ASI Observations

[4] Our event database is selected from the THEMIS ASI observations based on good viewing conditions and tractability of auroral brightening and expansions. For instrument description and geophysical map of THEMIS ASIs [see *Donovan et al.*, 2006b]. Table 1 gives a list of the identified events. Subject to one's criteria a few of the events may arguably be classified as pseudobreakups, but they are all characterized with noticeable poleward auroral expansion and definitive substorm features from corroborative ground-based and in-situ measurements (magnetometer, riometer, GOES, etc.). In all presentations of the images we assume an emission height of 110 km, and use the altitude-adjusted corrected geomagnetic coordinate to define magnetic latitude (MLAT) and longitude (MLON).

[5] The first event occurred on February 22, 2006. The auroral breakup was captured by the THEMIS ASI at Fort

[1]Space Science Branch, Canadian Space Agency, St-Hubert, Quebec, Canada.
[2]Department of Physics and Astronomy, University of Calgary, Calgary, Alberta, Canada.
[3]Finnish Meteorological Institute, Helsinki, Finland.
[4]Space Science Laboratory, University of California at Berkeley, Berkeley, USA.
[5]Athabasca University, Athabasca, Alberta, Canada.


0094-8276/08/2008GL033666$05.00

**Table 1.** List of Substorm Events From THEMIS ASI Observations[a]

| Date | Onset UT | Onset MLAT | Onset MLON | Wavelength | Growth Time |
|---|---|---|---|---|---|
| 2003/10/04 | 06:19:30 | 63.3° | −63−−50° | 0.8−1.5° | 18 s |
| 2005/11/28 | 10:12:00 | 65.0° | −97−−87° | 1.2−2.0° | 22 s |
| 2005/12/28 | 08:49:18 | 66.1° | −82−−69° | 1.6−2.4° | 11 s |
| 2006/01/27 | 10:02:24 | 66.9° | −99−−86° | 1.5−2.5° | 12 s |
| 2006/02/22 | 06:28:24 | 65.8° | −59−−44° | 1.7−2.2° | 9 s |
| 2006/04/15 | 07:04:18 | 64.8° | −60−−51° | 1.5−3.2° | 28 s |
| 2006/11/10 | 07:36:12 | 62.9° | −83−−74° | 1.1−1.6° | 24 s |
| 2007/03/13 | 05:07:45 | 64.5° | −50−−30° | 2.8−3.4° | 27 s |

[a]The onset MLON is estimated as the extent of breakup arc within 18 s of the onset (occasionally bound by the ASI FoV limitation). Wavelength is estimated from peak-to-peak longitudinal distances of intensification structures. Growth time is calculated from exponential fit of total auroral brightness.

Smith (FSMI) in 3 s cadence. Figure 1 shows a sequence of the images of the event. Prior to onset, the auroras are stationary and dark inside the field of view (FoV) of the ASI, with a predominantly azimuthally aligned quiet arc above 66° MLAT. The arc is found to be stable (with some slight equatorward motion) for ∼10 min during the late growth phase. Starting from 06:28:06 UT we see a few "spurs" sprouting (one at ∼−59° MLON is most visible) from the original arc to lower latitude, marking the first signature of the disruption of the growth phase arc. At 06:28:12 UT, another equatorward-extending "spur" at ∼−50° MLON also became evident. The "spur" grew in the next couple of frames into an equatorward displaced (marking with arrow in the 06:28:18 frame) arc segment in which the initial signature of the auroral intensification developed. The luminosity enhancement occurred both on the original arc and the new lower-latitude arc, whose formation over an extended azimuthal range becomes quite visible after 06:28:24. The overall auroral intensity was strongly enhanced in the following frames, marking substorm auroral breakup. The onset time for this event is estimated to be 06:28:24 ± 3 s. A key feature constituting the core interest of this paper is that the auroral intensification developed in distinct forms of azimuthally-spaced structures. For example, immediately following the onset, a number of discrete spots were quite conspicuous and spanned ∼1 h of longitude in the 06:28:30 frame, while the subsequent brightening appeared to be the clear wave-like auroral intensification within the same longitudinal extent. After 06:28:39 noticeable poleward auroral expansion merged the original and new arcs into an overall latitudinally broad structure. The color scale saturates at 06:28:42 but the embedded intensity wave structures can be clearly seen later in Figure 3a. The initial breakup is well within the

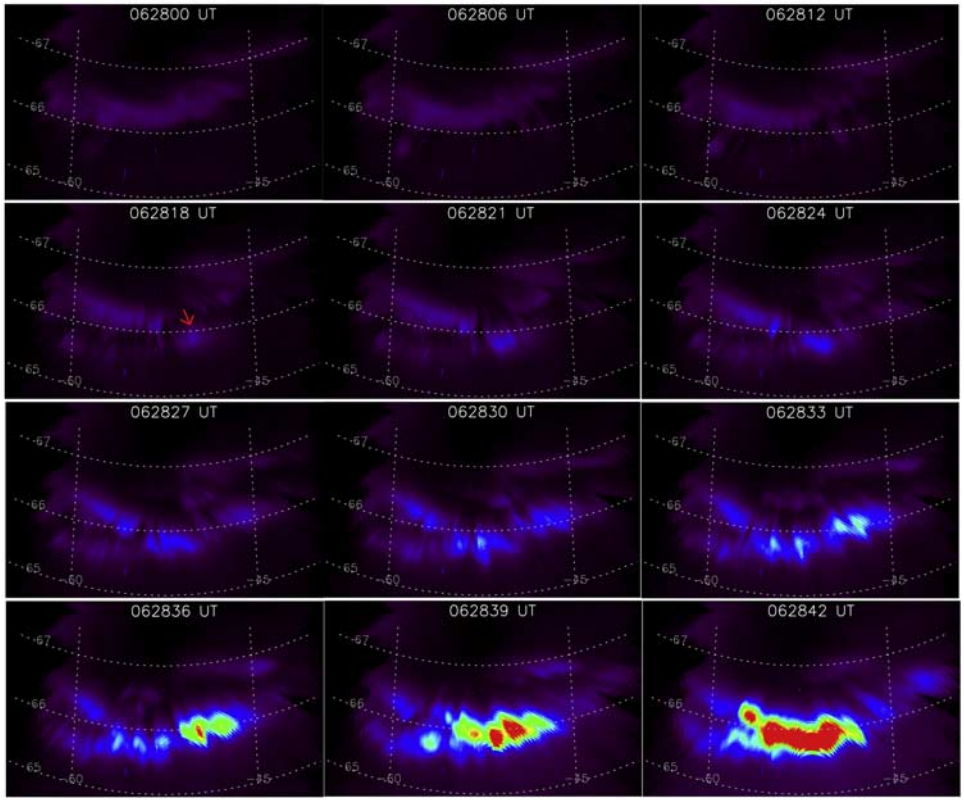


**Figure 1.** A sequence of THEMIS ASI images showing a substorm auroral breakup on February 22, 2006.

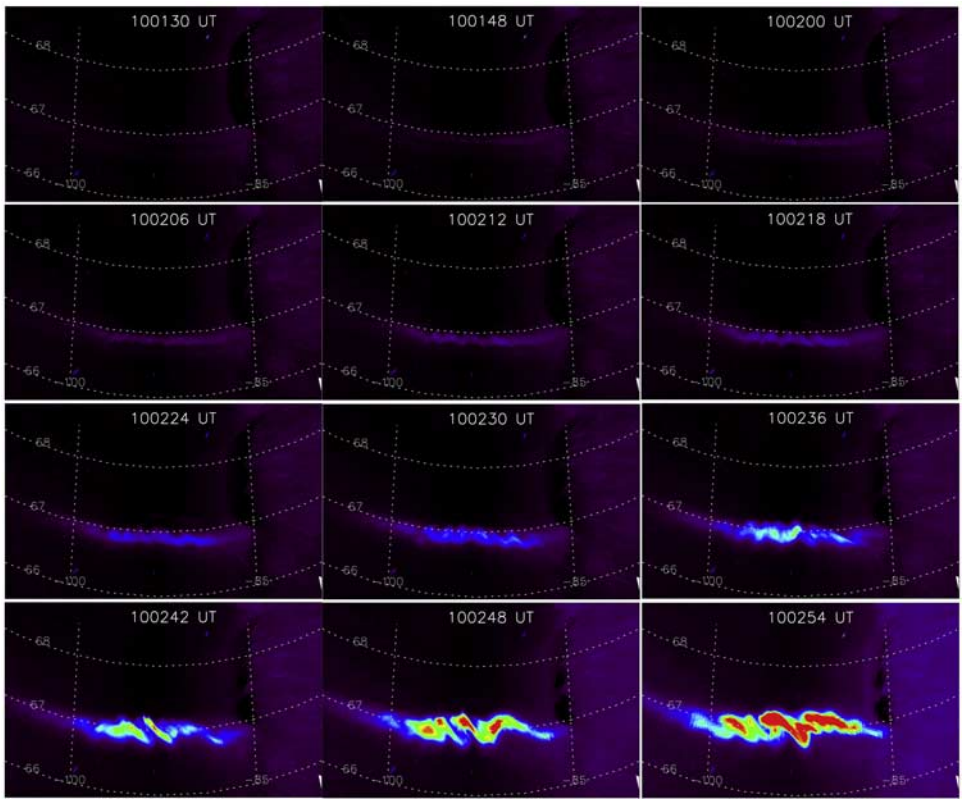


**Figure 2.** A sequence of THEMIS ASI images showing a substorm auroral breakup on January 27, 2006.

FoV of the FSMI ASI. We checked the nearby THEMIS ASIs and found no clue of substorm propagation into their FoVs until ~2 min after the initial onset.

[6] The second event occurred on January 27, 2006. Figure 2 shows a sequence of auroral images observed by the Fort Yukon (FYKN) ASI in 6 s cadence. The auroral breakup did not begin on any identifiable growth phase arc. It began, instead, on an arc that azimuthally formed just poleward of an existing faint arc that was probably inside the electron (isotropic) trapping boundary [*Deehr and Lummerzheim*, 2001], and slowly intensified ~1 min prior to the onset, similar to the observations of *Lyons et al.* [2002]. This newly formed arc was barely visible at 10:01:30 but became rather conspicuous by 10:02:00. Accompanying its gradual intensification are growing "ripples" in the new arc. Such wave-like modulation along the arc was quite noticeable by 10:02:18. The 10:02:24 frame is identified as the onset frame, from which we see near-simultaneous brightening over a ~10° longitudinal range. The intensification structures are embedded in the preexisting arc and also exhibited wave-like features as seen in 10:02:30 and 10:02:36 frames. From 10:02:36 to 10:02:42 UT we see that a part of the arc elevated in latitudes and became a tilted structure. Subsequently, the substorm auroras evolved into an undulation style featuring both latitudinally folded structures and longitudinally quasi-periodic structures. After 10:02:36 UT there was moderate auroral expansions towards both east and west but the major intensifications remained well inside the FYKN ASI FoV during the first few tens of seconds after the onset.

[7] For a better demonstration of the longitudinal wave-like structuring of breakup arc, we present in Figure 3 stack plots of latitudinally integrated emission brightness versus the MLONs in about 30 s around the EP onset for the two events presented above. To remove ambient noises and contaminations we have subtracted a "pre-onset" frame calculated as the average of all images in the 1-min interval prior to the onset. At the start of the event, the longitudinal distribution of auroral brightness is relatively structureless, but, in about 20 s, evolves into a quasi-periodic pattern. Although the two events described here are different in morphology, they both ultimately grow to have three luminosity peaks separated by 2–2.5° MLON and an overall bright arc spanning about ~1 h MLT. This behavior suggests that the underlying instability is similar for two events, featuring a characteristic longitudinal wave number $m$ = 140–180 of which the growth rate maximizes. Also plotted in Figure 3 is the temporal evolution of total substorm auroral brightness (integrated over both latitudes and longitudes). An exponential fit of the total brightness $I = a + b\ \exp(t/T_g)$ is made for each event, in which the e-folding growth time $T_g$ is found to be 9 s for event 1 and 12 s for event 2.

## 3. Discussion

[8] As a summary of the above two events, we have shown that the onset appears to occur over a longitudinally extended (10–15°) arc segment and characterized by distinct wave-like disruptions with a growth timescale of ~10 s. Examination of other THEMIS ASI onset events suggests that wave-like auroral activation is a quite common feature. Three events in our list were reported elsewhere by *Donovan et al.* [2006a, 2006b, 2008]. Readers are referred

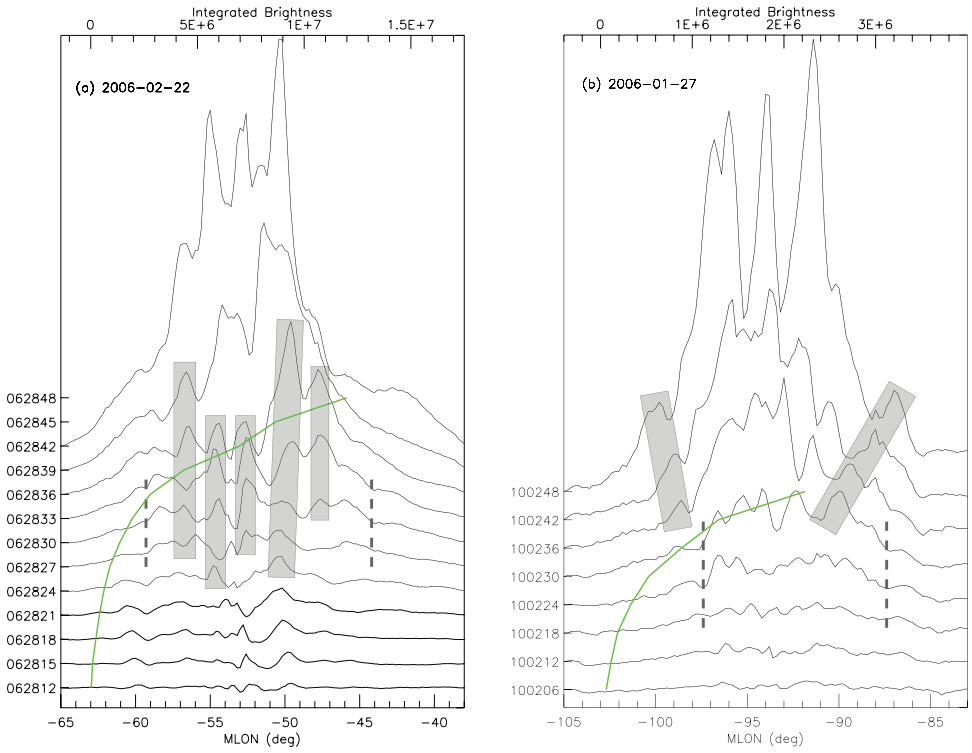


**Figure 3.** Stack plot of the longitudinally-integrated auroral brightness around the EP onsets for two events. Green curve denotes the temporal evolution of total auroral brightness (ticks on upper axis) with time (labeled on the left).

to Figure 5, Figure 8, and Figure 2B, in above three Donovan et al. publications respectively, to see remarkable similarities to events reported in this paper. Similar azimuthal structures were reported by *Elphinstone et al.* [1995] from Viking satellite images with ∼1 min resolution. With high-resolution THEMIS ASI observations we confirm that those azimuthal wave-like activations are intrinsic to the initial breakup process. The observations give strong hints of the existence of plasma instability waves at the NGPS in association with the substorm EP onset. In Table 1 we give the estimated wavelength and the growth timescale for all 8 events. The wavelength ranges between 1–3.4° MLON in the ionosphere, or roughly 800–2700 km at the NGPS. Noting that a 10-keV ion in a 10-nT equatorial magnetic field has a gyroradius on the order of 1000 km, the underlying instability of the auroral intensification is likely kinetic in nature, or a MHD instability significantly modified by the finite Larmor-radius effect.

[9] Dynamic auroral features occur both prior to and during the major brightening, which suggests that they are associated with separate but causally-related instability processes at two key stages of the substorm. The drift-Alfven-ballooning (DAB) instability [*Roux et al.*, 1991] and the cross-field current instability (CCI) [*Lui*, 1996] have received much attention in the last decade. The ballooning instability was considered by a number of researchers [*Liu*, 1997; *Cheng*, 2004] as the underlying mechanism of the "explosive growth phase" [*Ohtani et al.*, 1992], namely a rapid thinning of the near-Earth current sheet in ∼1 min prior to EP onset. *Cheng* [2004] computed the growth rate of an MHD ballooning instability and obtained a timescale ∼100 s at $L \sim 8\ R_E$. This is consistent with the results of *Saito et al.* [2008] based upon GEOTAIL observations that ballooning mode perturbations are identified ∼2 min prior to the dipolarization onset. The formation and gradual intensification of a new arc ∼1 min before the onset in event 2 is consistent with the above notion. Particularly, the growing "ripples" along the arc prior to the onset are likely an indication of the modulation of the cross-tail current via DAB [*Roux et al.*, 1991]. *Pu et al.* [1999] found that the DAB growth rate can be significantly boosted in the presence of fast earthward flows in the inner plasma sheet. In event 1, about 10–20 s before the onset a few "spurs" extending from the stable growth phase arc may be signatures of such earthward flows; consequently the development of the lower-latitude breakup arc was much faster in this event. When the current sheet is severely thinned to a thickness comparable or less than the thermal ion gyroradius, it may become unstable to several modes of CCIs that disrupt the cross-tail current. Potential role of pre-onset ballooning instability in leading to the CCI excitation was discussed by *Cheng* [2004]. There is substantial possibility that the DAB and CCI coexist to contribute to the azimuthally filamentary current structures and in turn our observations. Using 2D kinetic simulations, *Lui* [2004] reproduced the azimuthal structuring and disruption of the current sheet on a ∼10 s growth timescale; the obtained wavelength is comparable to our observations. However, due to the limitation of the numerical simulation *Lui* [2004] admitted that the attribution of the obtained wave-like structure to be CCI-driven was tentative. Direct and confirmative observational evidence of CCI modes at EP onset is still lacking so

far, and requires future investigations based upon coordinated in-situ measurements conjugate to the breakup arc.

[10] Another key observation resulting from the high-resolution capability of THEMIS ASI is the very fast azimuthal spreading of the initial auroral activation over 10–15° MLON within 10 s of the onset. For example, in event 1, seconds after the onset, a few azimuthally discrete spots spanning from about −59 to −44° MLON (marked in dashed lines in Figure 3a) are evident in the 06:28:30 frame. The subsequent brightening seems more or less confined within this extent and more interestingly, in a partially standing mode fashion. Note that a standing mode is usually implicative of waves trapped in a confined region [e.g., *Holter et al.*, 1995]. We highlight with gray bands in Figure 3a a few packets classified as "standing waves". Before the full growth of the wave packet, there may be several "valley-to-peak" variations with periods of ∼6 s, which we interpret to be the ionospheric Alfvénic resonator effect [*Lysak*, 1999]. After the ongoing current disruption has significantly changed the local conditions, the standing wave can no longer be sustained. The near-simultaneous onset behavior is also obvious for event 2. As shown in Figure 3b from 10:02:18 to 10:02:24 substantial brightening occurred within a range from −97.5 to −87.5° MLON. Subsequent expansion of the breakup arc was more moderate, hinted by the motion of the two side nodes at speeds of an order of magnitude slower (highlighted in gray bars, 0.16°/s for the eastern one and 0.1°/s for the western one) than the spreading of the initial brightening. The rapid expansion of the initial brightening in ∼10 s following the onset is also revealed in other events of our database. When this initial spreading stalls (e.g., in event 1 and work by *Donovan et al.* [2006a]), a more global expansion is found to resume 1–2 min later.

[11] If the substorm onset stems from a point source which then expands in space (which at first glance seems the case for event 1), and covers a ∼10° range in 10 s, it would map to an azimuthal speed of the order of ∼1000 km/s at the NGPS. A fast magnetosonic wave can barely reach this velocity in the local magnetosphere. If the expansion is attributed to a propagating drift wave [e.g., *Roux et al.*, 1991], the characteristic phase velocity would be of the order of the ion curvature/gradient drift speed, which is typically at most a couple of hundred km/s. While we cannot completely exclude the possibility of a "propagational" scenario from a point source, a careful examination of the image series makes us more disposed to the view that the initial breakup actually occurs simultaneously over an azimuthally extended segment of the current sheet that is preconditioned (possibly via ballooning mode) and subject to sudden disruptions. The instability growth rate is spatially dependent, such that the brightening of discrete "spots" or fragments may exhibit an apparent time-lapsed emergence (thus a "propagational" illusion) due to the threshold effect discussed by *Liang et al.* [2005] (see their Figure 13).

[12] We have also considered the possibility that the auroral breakup is a result of mid-tail reconnection. It is difficult to definitively establish the presence or absence of reconnection based solely on auroral data. In the event with corresponding in-situ observations [*Donovan et al.*, 2008] no signature of reconnection was revealed. We have checked for auroral streamers that are often associated with bursty bulk flows for the 8 events in our database and were unable to find any in the minutes preceding the onset. Therefore the scenario in which substorm EP onset arises directly from the reconnection or as an immediate consequence of reconnection-driven fast flows is not evidenced within the context of our observations. We emphasize though, all our events are found as either isolated or the leading one followed by subsequent activation that is possibly reconnection-driven [*Donovan et al.*, 2008].

## 4. Conclusion

[13] Although intensification of a preexisting auroral arc has long been recognized as the key substorm EP feature, it was not until very recently that we could make systematic observations of the details of this intensification with the high enough spatiotemporal resolution via THEMIS ASIs. In this paper, we focused on a few tens of seconds around the substorm EP onset and found two important details of arc intensification: (a) the pattern of intensification is neither uniform nor random, but features a wave-like action with a high longitudinal wave number between 100 and 300; (b) the auroral breakup spreads rapidly to a ∼1 h longitudinal extent within ∼10 s of the onset while the subsequent expansion is much slower or stalls. The two pieces of observations hint that the breakup is due to simultaneous destabilization of a wave mode over a finite azimuthal extent of the current sheet. We have considered a few possible mechanisms behind the observation. Tentatively we suggest that the ballooning mode might be responsible for setting up an extremely thinned current sheet segment, whose destabilization via an indeterminate but likely kinetic instability (e.g., CCI), corresponds to the wave-like disruption of auroral arc reported in this paper.

[14] **Acknowledgments.** THEMIS was developed under the NASA Explorer Program. Funding for THEMIS GBO operation and data retrieval was provided by the CSA. This study is supported by NSERC and CSA.

## References

Cheng, C. Z. (2004), Physics of substorm growth phase, onset, and dipolarization, *Space Sci. Rev.*, *113*, 207–270.

Deehr, C., and D. Lummerzheim (2001), Ground-based optical observations of hydrogen emission in the auroral substorm, *J. Geophys. Res.*, *106*, 33–44.

Donovan, E., et al. (2006a), The azimuthal evolution of the substorm expansive phase onset aurora, in *Proceedings of ICS-8*, edited by M. Syrjäsuo and E. Donovan, pp. 55–60, Univ. of Calgary, Calgary, Alberta, Canada.

Donovan, E., et al. (2006b), The THEMIS all-sky imaging array-system design and initial results from the prototype imager, *J. Atmos. Sol. Terr. Phys.*, *68*, 1472–1487.

Donovan, E., et al. (2008), Simultaneous THEMIS in situ and auroral observations of a small substorm, *Geophys. Res. Lett.*, doi:10.1029/2008GL033794, in press.

Elphinstone, R. D., et al. (1995), Observations in the vicinity of substorm onset: Implications for the substorm process, *J. Geophys. Res.*, *100*, 7937–7969.

Holter, Ø., et al. (1995), Characterization of low frequency oscillations at substorm breakup, *J. Geophys. Res.*, *100*, 19,109–19,119.

Liang, J., et al. (2005), Substorm dynamics revealed by ground observations of two-dimensional auroral structures on 9 October 2000, *Ann. Geophys.*, *23*, 3599–3613.

Liu, W. W. (1997), Physics of the explosive growth phase: Ballooning instability revisited, *J. Geophys. Res.*, *102*, 4927–4931.

Lui, A. T. Y. (1996), Current disruption in the inner magnetosphere: Observations and models, *J. Geophys. Res.*, *101*, 13,067–13,088.

Lui, A. T. Y. (2004), Potential plasma instabilities for substorm expansion onsets, *Space Sci. Rev.*, *113*, 127–206.

Lyons, L. R., I. O. Voronkov, E. F. Donovan, and E. Zesta (2002), Relation of substorm breakup arc to other growth-phase auroral arcs, *J. Geophys. Res.*, *107*(A11), 1390, doi:10.1029/2002JA009317.

Lysak, R. L. (1999), Propagation of Alfvén waves through the ionosphere: Dependence on ionospheric parameters, *J. Geophys. Res.*, *104*, 10,017–10,030.

Mende, S. B., V. Angelopoulos, H. U. Frey, S. Harris, E. Donovan, B. Jackel, M. Syrjaesuo, C. T. Russell, and I. Mann (2007), Determination of substorm onset timing and location using the THEMIS ground based observatories, *Geophys. Res. Lett.*, *34*, L17108, doi:10.1029/2007GL030850.

Ohtani, S., K. Takahashi, L. J. Zanetti, T. A. Potemra, R. W. McEntire, and T. Iijima (1992), Initial signatures of magnetic field and energetic particle fluxes at tail reconfiguration: Explosive growth phase, *J. Geophys. Res.*, *97*, 19,311–19,324.

Pu, Z., et al. (1999), Ballooning instability in the presence of a plasma flow: A syntheses of tail reconnection and current disruption models for the initiation of substorms, *J. Geophys. Res.*, *104*, 10,235–10,248.

Roux, A., S. Perraut, P. Robert, A. Morane, A. Pedersen, A. Korth, G. Kremser, B. Aparicio, D. Rodgers, and R. Pellinen (1991), Plasma sheet instability related to the westward traveling surge, *J. Geophys. Res.*, *96*, 17,697–17,714.

Saito, M. H., Y. Miyashita, M. Fujimoto, I. Shinohara, Y. Saito, K. Liou, and T. Mukai (2008), Ballooning mode waves prior to substorm-associated dipolarizations: Geotail observations, *Geophys. Res. Lett.*, *35*, L07103, doi:10.1029/2008GL033269.

V. Angelopoulos, H. U. Frey, and S. B. Mende, Space Science Laboratory, University of California at Berkeley, Berkeley, CA 94720, USA.

M. Connors, Athabasca University, Athabasca, AB, Canada, T3G 2Z8.

E. F. Donovan and B. Jackel, Department of Physics and Astronomy, University of Calgary, Calgary, AB, Canada T2N 1N4.

J. Liang and W. W. Liu, Space Science Branch, Canadian Space Agency, 6767 Route de l'Aeroport, St-Hubert, QC, Canada J3Y 8Y9. (jun.liang@space.gc.ca)

M. Syrjäsuo, Finnish Meteorological Institute, FI-00101 Helsinki, Finland.